Layered, Erasable Polymer Multilayers Formed by Hydrogen-Bonded Sequential Self-Assembly

ARTICLE *in* MACROMOLECULES · DECEMBER 2001

Impact Factor: 5.8 · DOI: 10.1021/ma011346c

1 AUTHOR:

Svetlana Sukhishvili
Stevens Institute of Technology
134 PUBLICATIONS **4,811** CITATIONS

Layered, Erasable Polymer Multilayers Formed by Hydrogen-Bonded Sequential Self-Assembly

Svetlana A. Sukhishvili

Department of Chemistry and Chemical Biology, Stevens Institute of Technology, Hoboken, New Jersey 07030

Steve Granick*

Department of Materials Science and Engineering, University of Illinois at Urbana−Champaign, Urbana, Illinois 61801

Received July 30, 2001

ABSTRACT: Robust multilayers can be formed on solid surfaces, and subsequently destroyed by changing the environmental conditions, by the layer-by-layer sequential assembly of monomolecular films of a polyacid and polybase from aqueous solution. Interlayer hydrogen bonding produces stable multilayers up to the point where altered pH or other environmental stimulus introduces an unacceptably large electrical charge within them. This is demonstrated for the polyacids poly(acrylic acid), PAA, and poly(methacrylic acid), PMAA, and for the polybases poly(vinylpyrrolidone), PVPON, and poly(ethylene oxide), PEO, in D_2O. The adsorption was quantified by Fourier transform infrared spectroscopy in attenuated total reflection (FTIR-ATR). The ratio between suppressed ionization of the carboxylic groups within the film and their ionization in solution, as directly measured by FTIR-ATR, was used to estimate the fraction of hydrogen-bonded carboxylic groups; this was ∼0.5 in PVPON/PMAA but only ∼0.1 in the PEO/PMAA system, though the dielectric environments appeared to be similar. The critical pH, at which these hydrogen-bonded layers disintegrated, was controlled by a balance of internal ionization and a fraction of carboxylic groups that formed hydrogen bonds with either PVPON or PEO. The critical point was at pH = 6.9 for the PVPON/PMAA films (relatively strong hydrogen bonding), but pH = 4.6 for the PEO/PMAA films (in which a smaller fraction of segments participated in hydrogen bonding). It was even less, pH = 3.6, in the PEO/PAA system, which contained a larger proportion of ionized groups at a given pH owing to the higher acidity of PAA. As a second avenue to control the stability of these multilayer films, ionic strength was varied systematically. In the PEO/PMAA system, the multilayers were stable up to pH = 4.6 in the environment of 10 mM ions (this ionic strength resulted from the buffer solution to control pH), but the multilayers were stable up to higher pH, pH = 5.15, when 0.4 M NaCl was added. The reason is that a higher ionic strength reduced the intensity of electrostatic repulsion between a given number of ionized groups within the multilayer assembly. A slight weakening of stability with decrease of molecular weight was observed (these experiments concerned the PVPON system) as expected from fewer hydrogen bonds per molecule. Finally, experiments with added rhodamine 6G dye showed that dye or drug molecules can be incorporated into such multilayers and then released as needed at preselected conditions—a feature that may be used in drug release devices.

Introduction

Building up of organic multilayer films by layer-by-layer sequential adsorption of charged polymers on solid substrates has proven to be an experimentally simple and versatile method to produce nanoscopically structured macroscopic films.[1−7] First introduced by Decher in 1991,[8] this technique was quickly recognized as a highly useful way for self-assembly of organic and inorganic substances of diverse nature, including proteins, DNA, inorganic sols, and clay particles.[9] The produced layered films of self-assembled molecules have found multiple applications in the fields of biosensors, light-emitting diodes, nonlinear optical devices, and permselective gas membranes.[10−13] Following a recent example of Möhwald and colleagues as concerns electrostatic self-assembly,[14] the method was also found to apply to small micron-sized down to nanosized particles, thereby affording a method to encapsulate small particles within these coatings. These examples of layer-by-layer self-assembly rely on the electrostatic attraction between molecules of opposite charge.

Fewer studies concern "weak" polyelectrolytes, whose charge responds to the local electrostatic environment by the chemical equilibrium known as ionization (see below). However, a considerable knowledge exists on how to use hydrogen bonds and hydrophobic forces to induce complexation of synthetic water-soluble compounds with other water-soluble polymeric partners[15−17] or hydrogels.[18] Hydrogen bonding is also used extensively to induce supramolecular ordering in other synthetic polymer systems[19−21] and is crucial to such very basic processes of life as protein synthesis, specific protein recognition, or DNA duplication. As we will discuss in detail in this paper, the knowledge about hydrogen-bonding interactions that arose in these fields of study is also potentially useful in the field of self-assembly at surfaces. When applied to self-assembly at surfaces, the use of weak polyelectrolytes widens the window for manipulation of molecular organization beyond that achievable when using polymers whose charge density is fixed.[3,22−27]

Rubner and co-workers initiated the study of layer-by-layer assembly through hydrogen bonding of polyaniline,[28] though a system-dependent interpretation was proposed at that time. Other studies that employ hydrogen-bonded self-assembly have also appeared

10.1021/ma011346c CCC: $22.00
Published on Web 12/05/2001

recently.[29−32] In a recent communication, we further demonstrated that hydrogen-bonded self-assembled multilayers can be "erased" by intentionally applied environmental stimuli,[31] and this has been developed by Schlenoff and co-workers.[32] Here we report a full study of our preliminary communication.[31]

Specifically, this study employs the idea of hydrogen-bonding-driven self-assembly to produce polymer multilayers on solid substrates. We show systematically that (1) synthetic polymers, such as poly(carboxylic acid) and polymers containing electron-donating functional groups, can be assembled into multilayers by sequential adsorption and (2) such films can be then destroyed at will by ionization of carboxylic groups, either by changing pH/ionic strength or by applying an external electric field. Our findings show an avenue for novel applications of polymer multilayers, possibly ranging from self-destroying materials for temporary protection to new materials for drug delivery.

Experimental Section

A. Materials. All polymers were used as received. Poly(ethylene oxide) (PEO) was purchased from Pressure Chemical. The weight-average molecular weight was M_w = 594 000 g mol^{-1}, and the ratio of weight-average to number-average molecular weight is stated to be M_w/M_n = 1.03. Special care was taken to ensure complete dissolution of PEO since undissolved PEO was reported as a possible source of aggregates in PEO solution.[33] The variation of a literature recipe[34,35] involving careful solution preparation was used. The PEO was dissolved in acidic D_2O at 55 °C with gentle shaking and then filtered through a 0.22 μm pore size cellulose acetate filter.

Poly(vinylpyrrolidone) (PVPON) samples with average molecular weights ∼1 300 000 and ∼ 55 000 g mol^{-1} were purchased from Aldrich.

The sodium salt of poly(methacrylic acid) (PMAA) with M_w = 327 000 and M_w/M_n = 1.03 was received from Polymer Standards Service (Germany).

Poly(acrylic acid) (PAA) was purchased from Polymer Source (Canada) and had the following molecular weight parameters: M_w = 164 000 and M_w/M_n = 1.13.

Poly(4-vinylpyridine) (PVP) sample with M_w = 34 200 g mol^{-1} and M_w/M_n = 1.23 was purchased from Polymer Source, Québec, Canada. This sample was quaternized with ethyl bromide using well-established methods[36,37] to obtain a polymer with 98% of pyridinium units as determined by infrared spectroscopy. We refer below to quaternized PVP as QPVP.

To reduce overlap of the infrared (IR) spectra of the amide I band with the strong water band, we used as solvent D_2O with 99.9% isotope content. This was purchased from Cambridge Isotope Laboratories and was used as received. The acidity was therefore determined by deuterium rather than hydrogen ions. A purist, who measures the D^+ concentration, might refer to this measure as pD rather then pH. The discussion below shall nonetheless refer to it as pH, because this terminology is more common. Similarly, the discussion will employ the term "hydrogen bonding", not "deuterium bonding".

To control pH and ionic strength, concentrated HCl and the inorganic salts $Na_2B_4O_7{\cdot}10H_2O$, Na_2HPO_4, $NaH_2PO_4{\cdot}H_2O$, and NaCl (General Storage, pure grade) were used as received.

The H_2O used for glassware cleaning was double-distilled and further purified by passage through a deionizing Milli-Q System (Millipore).

B. Pretreatment of the ATR Crystal. Multilayer films were deposited on a variety of substrates, including (1) hydrophilic Ge crystal (its specifications are given below) which was oxidized using the procedure described elsewhere[38] and (2) Ge crystal which was rendered hydrophobic by allowing hydrolyzed octadecyltriethoxysilane to self-assemble on the surface.[39]

In case 1, multilayers could not be deposited on the bare hydrophilic surface of Ge crystal directly; adhesion to it of the polymers used in this study was weak. To enhance the adhesion of polymers to the substrate, the surface was first modified by allowing QPVP to adsorb from an 0.2 mg/mL solution at pH = 9.2. Adsorption occurred, probably due to Coulumbic attraction to the surface at this high pH. After waiting 40 min, the amount adsorbed reached a saturated value of ∼1.5 mg m^{-2}, and polymer solution was replaced by a pure buffer. The procedure yielded the surface of the Ge crystal covered with the layer of cationic molecules carrying permanent electrical charge. Then the desired solution of PMAA or PAA (1 mg/mL in the same buffer solution) was added. The polymer solution was then replaced momentarily by the pure buffer at the same pH and finally by a D_2O solution at much lower pH = 2 (pH was controlled by added HCl). The saturated amount of poly(carboxylic acid) deposited at this step, ∼0.5−0.7 mg m^{-2}, was consistent with a charge compensation mechanism of the adsorption. Before this substrate (containing the two-layer pretreatment) was used for multilayer deposition, a buffer solution containing 0.01 M HCl was injected into the liquid cell.

In case 2, adhesion of polyacids to a hydrophobically modified Ge surface at pH = 2 was strong enough so that it was not necessary to modify the surface with a precursor film.

C. Deposition of the Hydrogen-Bonded Multilayers. Multilayers were then deposited in the layer-by-layer fashion. The protocol for multilayer deposition was slightly different from the technique of alternate dipping that is commonly used for the multilayer deposition. In a typical route, 1 mg/mL solution of polymer A (PAA or PMAA) was allowed to adsorb to the surface of modified Ge crystal at pH 2 for 20 min, and after that polymer solution was replaced by the buffer without polymer. Polymer A did not desorb into the pure buffer (neither at the same nor at different pH) or after the subsequent adsorption of polymer B (PVPON or PEO). On top of polymer A, polymer B was then deposited in a similar way, and the deposition cycle was repeated. Examples are shown in the Results section.

D. Methods. 1. FTIR-ATR Measurements. The layer-by-layer adsorption was monitored by infrared spectroscopy using attenuated total reflection. Infrared spectra were collected using a Biorad FTS-60 Fourier transform infrared spectrometer (FTIR) equipped with a broad-band mercury cadmium telluride detector. The attenuated total reflection (ATR) optics and the thermostated home-built adsorption cell were placed in a nitrogen-purged compartment external to the FTIR spectrometer, as described previously.[38]

The temperature, regulated by circulation of water through a jacket surrounding the metal enclosure of the ATR cell, was 25.0 °C. The ATR surface was a rectangular trapezoidal Ge crystal of dimension 50 mm × 20 mm × 2 mm (Harrick Scientific) whose beam entrance and exit surfaces were cut at 45°. The methods to controllably oxidize the crystal surface and to clean the cell elements were described elsewhere.[38] These methods of surface preparation yielded adsorption measurements that were quantitatively reproducible from experiment to experiment.

Interferograms were collected with 4 cm^{-1} resolution, and the number of averaged scans was 512. To obtain the absorbance spectra analyzed below, each interferogram was ratioed to a corresponding background, measured for the same ATR cell with the same D_2O buffer solution. Two types of spectra were obtained: (1) spectra of the top deposited polymer layer and (2) spectra of the whole polymer film deposited on the ATR crystal. In case 1, the background signals were taken with the ATR crystal covered with the multilayer films produced in the previous cycle of polymer deposition. In case 2, the background spectra were obtained with the bare ATR crystal or the ATR crystal covered with the precursor film. The integrated peaks, inferred amount adsorbed, and inferred ionization from these two approaches were consistent within 3%.

The infrared absorption peaks were integrated using curve fitting of the absorption peaks. The most consistent results were obtained when 90% of the peaks were assumed to be

Table 1

polymer	absorbance band, cm^{-1}	band assignment	calibration constant, abs units $m^2\ mg^{-1}$
PMAA	sum of 1701 and 1554 cm^{-1} bands	CO and COO stretch	0.128
PAA	sum of 1706 and 1570 cm^{-1} bands	CO and COO stretch	0.234 (Na^+ salt)
0.294 (protonated form)			
PEO	several 1000−1200 cm^{-1} bands with peak intensity at 1079 cm^{-1}	COC stretch region[a]	0.203
PVPON	1647 cm^{-1}	CON stretch	0.251
QPVP	1643 cm^{-1}	pyridinium ring in-plane stretch	0.028

[a] For details see ref 60.

Gaussian and 10% to be Lorenzian. The peak centers and bandwidths were not fixed, but the results of the curve fitting were carefully checked for consistency in these parameters. In curve fitting, a baseline correction was performed to the raw spectra.

Owing to the large penetration depth of the evanescent wave relative to thickness of the adsorbed layer (for example, the penetration depth of the evanescent wave was 0.41 μm at 1643 cm^{-1} for the Ge crystal that we used), if the measurements were performed in the presence of polymer solutions, the signal included contributions from the polymer solution in addition to those from the adsorbed polymer layers. Their respective contributions were easily separated when after each adsorption cycle the polymer solution was replaced by the pure buffer; while doing so, the adsorbed polymer molecules remained irreversibly bound to the surface of the substrate. The contribution of the solution value was roughly 3−10% of the total signal for a solution concentration of 1 mg mL^{-1}.

In most experiments, the penetration depth of the evanescent wave was large relative to the thickness of the multilayers, and it was not necessary to correct data for the decay of electric field with the distance from the surface of the crystal. A simple calculation showed that this assumption held up to the thickness of the film of about ∼500 Å. Dry, the adsorbed amount would be about 50 mg m^{-2}. (In this estimate, a refractive index of 1.48 and density of 1 g cm^{-3} were assumed.) For films thicker than 500 Å, the measured intensity was corrected for decreasing intensity of the evanescent wave within the probed volume. The correction did not usually exceed 25%. For example, it was 20% for the films with 100 mg m^{-2} total mass deposited.

The adsorbed amount was calibrated from the absorptivity of polymers in bulk solution, measured independently, as summarized in more detail elsewhere.[38,40] In brief, polymer solutions of known concentrations were brought into contact either with a bare surface of the Ge crystal or with a saturated adsorbed layer, so that these surfaces could be considered as essentially nonadsorbing with respect to the possibility of adsorption. From the slope of the integrated absorbance for the corresponding bands and the known value of penetration depth, the calibration constants to infer the adsorbed amounts were obtained; they are listed in Table 1 for the various polymers used in multilayer deposition.

2. Ellipsometric Measurements. Measurements were performed on dry films in air using a Gaertner model L 116C ellipsometer with He/Ne laser (632 nm) illumination at a 70° angle of incidence. A refractive index of 1.48 for the dry film was assumed. The thickness of the multilayers was measured after measuring the real and imaginary parts of the refractive index of the Ge crystal, n_s and K_s.

Results and Discussion

A. Sequential Growth of PVPON/PMAA and PEO/PMAA Multilayers. 1. Kinetics of Deposition of Multilayers. Growth of the multilayers was followed by in situ ATR-FTIR experiments. Details will be described in the following section. The mass deposited grew quickly and approached its steady state after a time span of 10−15 min. At longer times, adsorption continued to grow with almost linear increments of about ∼3% of mass increase per hour for at least another 2 h. This slower kinetics had evidently a different origin than transport of PVPON molecules to the surface. It is interesting to notice that similar long-time equilibration effects are also seen for the adsorption of nonpolar polymers and polyelectrolytes[41,42] at solid surfaces. The seeming generality of the observations is tantalizing and suggests that they are possibly rooted in the same physical phenomenon. We simply ignored this slower part in the kinetics of deposition, as it was not the point of this study. The adsorption was usually interrupted within 20 min, after the quick adsorption step was completed, and the cell was filled with a buffer solution containing 0.01 M HCl. Deposition of PMAA, PAA, and PEO followed a similar kinetics pattern.

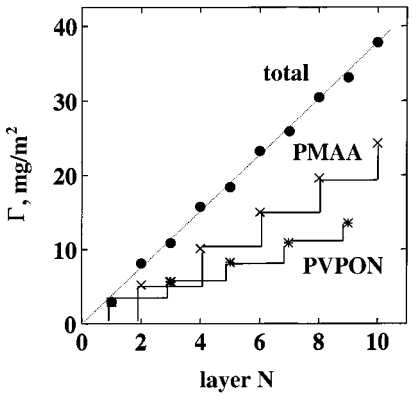

Figure 1. Illustration of layer-by-layer deposition of 10 layers in the PVPON/PMAA system. Mass deposited after 30 min of self-assembly from 1 mg mL^{-1} solution is plotted against layer number for PMAA (crosses) and PVPON (stars) and for the total mass deposited (circles). The spectra were taken in buffered D_2O, which contained 0.01 M HCl. The substrate was a Ge crystal modified with a primer layer (see text).

2. Self-Assembly of PVPON/PMAA Multilayers. The fidelity of layer-by-layer deposition of poly(methacrylic acid) and poly(vinylpyrrolidone) was demonstrated in the in situ ATR-FTIR experiment. Mass deposited within a multilayer in a sequence of 10 steps of layer-by-layer assembly is plotted in Figure 1. One observes that the same incremental mass of PVPON and PMAA was adsorbed at each step of layer-by-layer deposition. This incremental mass increase was 2.7 mg m^{-2} for PVPON and 4.4 mg m^{-2} for PMAA, suggesting 2.1 times molar excess of PMAA in the multilayer. It seems surprising at the first glance that the molar balance of polymers was different from unity. Similar stoichiometry was however found for complexation of poly(carboxylic acid)s with PVPON in solution[43,44] and is probably associated with the strong proton-accepting properties of the carbonyl group in the PVPON molecule, which could be able to form two hydrogen bonds with carboxylic groups of PMAA. It is also evident that

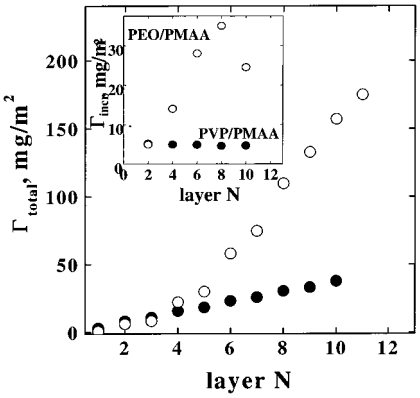

Figure 2. Comparison of layer-by-layer deposition in PVPON/PMAA and PEO/PMAA systems. Inset shows the incremental mass growth within each layer. Conditions are the same as in Figure 1.

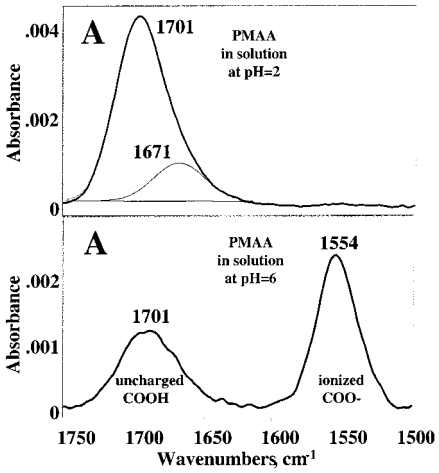

Figure 3. Infrared absorption spectrum of poly(methacrylic acid), PMAA, at concentration 10 mg mL^{-1} in buffered D_2O solution at pH = 2 (panel A) and pH = 6 (panel B). The absorption bands at 1701 and 1554 cm^{-1} correspond to not ionized and ionized forms of carboxylic groups in PMAA molecule. They were used to determine the degree of ionization and amount of PMAA deposited within a multilayer (see text). The adsorption modes of the asymmetric peak at 1701 cm^{-1} are shown as dotted lines. The composition of the buffer solution was 0.01 M HCl (panel A) or 0.01 M phosphate buffer (panel B).

the driving force for self-assembly evidently competed favorably with the known intramolecular association of carboxylic acid units within single PMAA molecules at low pH.[45]

Ancillary ellipsometric measurements showed that the average dry layer thickness in this experiment was 3.5 nm per layer (2.6 nm per PVPON layer, 4.4 nm per PMAA layer). Knowing that the density of the dry organic film is approximately 1 g cm^{-3}, this amounts to good agreement with the IR measurements of the sequential mass deposition into the multilayer.

It is important to notice that the thickness of the PVPON layer deposited in each successive cycle was the same with longer PVPON molecules ($M \sim 1\,300\,000$ g mol^{-1}) and with much shorter PVPON molecules ($M \sim 55\,000$ g mol^{-1}), although R_G in solution was 5 times different. The polymer molecules evidently spread at the surface at the time of deposition, due to attractive intermolecular interactions between PVPON and PMAA groups. Note that similar "spreading" or "zipping" of the molecules also lies at the heart of complexation of polymers in solution. It presents a necessary mechanism for the growth of cooperative sequences of associating units, the major contribution to stability of interpolymer complexes.[45,46] This picture of flattening or polymers at the time of adsorption is consistent with the fact that a large fraction of functional groups in the PVPON and PMAA molecules would take part into intermolecular hydrogen bonding; these data are presented below.

3. PEO/PMAA Multilayers. In this section we began to vary chemical makeup of the polymer molecules used. Poly(ethylene oxide), PEO, was another evident candidate because of its known ability to produce stable interpolymer complexes with poly(carboxylic acid)s at acidic pH in solution.[15−17,47,48] Figure 2 shows that association between PEO and PMAA molecules can be also used to produce macromolecular assemblies on a solid support. Two points are evident in Figure 2. First, the multilayers grew in a strikingly different way than in the PVPON/PMAA system. Instead of consistent differential growth of mass deposited in each cycle, one sees an avalanche-like or runaway growth of mass adsorbed with increasing layer number. After eight cycles of deposition, the incremental growth of the deposited mass was as high as 30−50 mg m^{-2}, about 10 times larger than in the PVPON/PMAA system. Another point is that after the amount deposited in each cycle and/or total mass of polymers in the multilayers approached a certain limit (∼50 mg m^{-2} per layer in this experiment) subsequent layer growth was then inhibited, probably due to mechanical failure of the film. Thereafter, the amount of polymers deposited in each cycle severely decreased.

The imperfect growth of multilayers in this system contrasts with the robust deposition of the PVPON/PMAA multilayers. We hypothesize that irregular deposition stemmed from weaker complexation between PEO and PMAA molecules. This fact is widely known[49,50] and was also confirmed in this paper by direct measurement of the degree of hydrogen bonding in the film (see below). Weaker binding between PEO and PMAA molecules might produce a larger number of defects in the PEO/PMAA structure and facilitate roughening of the surface. Indeed, inhomogeneous "patchy" surfaces were seen in AFM images of the dry PEO/PMAA films (these data are not included).

Note that despite the runaway effect, the amount of polymer deposited from solution was always strictly controlled by the amount of polymer in the layer below and approached a definite limiting value.

B. FTIR Analysis. 1. Representative Spectra of PMAA. Figure 3 shows infrared spectra of PMAA taken at two different pH, pH = 2 and 6. Infrared absorbance is plotted against wavenumber. In these experiments, solutions of PMAA with known concentration were exposed either to the bare surface of Ge crystal (at pH = 6) or to this surface containing a saturated adsorbed layer of PMAA (at pH = 2). Since PMAA acid did not adsorb onto the native surface of Ge crystal, in both cases, the measured absorbance originated only from molecules free in solution.

The spectra show a strong absorption band at 1701 cm^{-1} associated with the stretch vibrations of the uncharged form of carboxylic groups and, when charged, a second band at 1554 cm^{-1} from the asymmetric stretching vibrations of the carboxylate groups (ν_a, COO^-). With varying pH, the relative intensities of the 1554 and 1701 cm^{-1} peaks changed while the total intensity did not. This allowed us not only to calibrate

the amount adsorbed (see Experimental Section) but also to calculate the degree of ionization of PMAA molecules at various pH.

It is interesting to notice that frequencies much higher that 1700 cm^{-1} are usually observed for a monomeric uncharged form of the carboxylic group.[51] At the same time, a vibrational peak centered around 1700 cm^{-1} is commonly observed in melts of poly(carboxylic acid)s, presumably due to the associated or dimerized form of carboxylic groups.[52,53] It is possible that association of carboxylic groups still persists in the hydrated form of the PMAA molecules.[45,53] It is also reasonable to believe that shift of the C═O vibrational bands to lower wavenumbers is caused by perturbations due to hydrogen bonding with D_2O molecules. Solvent effects on vibrational shifts are widely known.[54] We were unable to distinguish between these two contributions at this point.

The shape of the 1701 cm^{-1} band is clearly asymmetric (Figure 3A), with noticeable spectral broadening at the lower frequencies. Similar spectra shapes were reported elsewhere.[55] The origin of these lower-energy vibrations is unclear. Hydrogen bonding between more than two carboxylic groups was recently proposed.[53] Following another argument, the peak broadening might be rooted in short-range interactions of carbonyl dipoles, and the asymmetry of the peak might be produced owing to higher probability of antiparallel arrangement of the dipoles.[56] To account for this low-wavenumber peak broadening, we introduced in curve fitting the possibility of a 1671 cm^{-1} vibrational band; the exact position of the peak was determined in the second-derivative analysis of the band shape. As shown in Figure 3A, the spectrum of PMAA in solution can be successfully fitted with two peaks located at 1701 and 1671 cm^{-1}. The most consistent results were obtained when the peak shapes were assumed to consist of 90% Gaussian and 10% Lorenzian contributions, and the width of the peaks was fixed at 40 cm^{-1}. The peak centered at 1671 cm^{-1} comprised about 20−22% of the total intensity of carbonyl vibrations in the uncharged form of the PMAA molecules.

Infrared spectra of PAA in the carbonyl region were similar to spectra of PMAA, but with the vibrational peaks shifted by ∼7 cm^{-1} to higher wavenumbers. The peak for carbonyl stretching vibrations could be fitted well by one strong peak centered at 1708 cm^{-1} and a weaker peak centered at 1678 cm^{-1}. The lower frequency peak comprised about 25% of the total intensity in the carbonyl region. The asymmetric stretching vibrations of the charged form of the carboxylic groups in PAA also emerged at significantly higher frequency, at 1570 cm^{-1} compared to 1554 cm^{-1} in the PMAA molecules. The origin of these shifts is not understood at present.

2. Representative Spectra of PVPON. The spectrum of poly(vinylpyrrolidone), PVPON, in solution in the1600−1700 cm^{-1} region is shown in Figure 4. It has a broad band centered at 1647 cm^{-1}, which is usually assigned to the carbonyl stretch (CON stretch) vibrations of the pyrrolidone ring. The position of this peak was shifted to lower frequencies than for the previously reported stretch frequency of C═O in poly(vinylpyrrolidone) melts,[57−59] presumably owing to perturbations of the carbonyl vibrations due to hydrogen bonding with water. Second-derivative analysis showed that this broad band could be decomposed into two strong bands

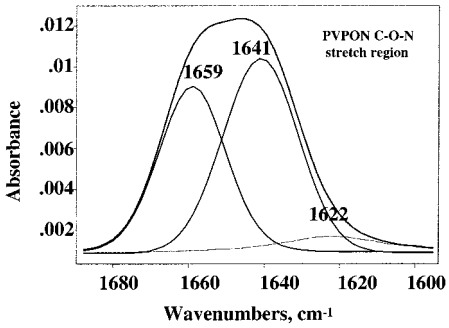

Figure 4. Infrared absorption spectrum of poly(vinylpyrrolidone), PVPON, at concentration 10 mg mL^{-1} in buffered D_2O solution at pH = 2 and its spectral decomposition into the constituent adsorption modes. The adsorption mode centered at 1622 cm^{-1} was used to infer the degree of hydrogen bonding. The pH = 2 was produced by added 0.01 M HCl.

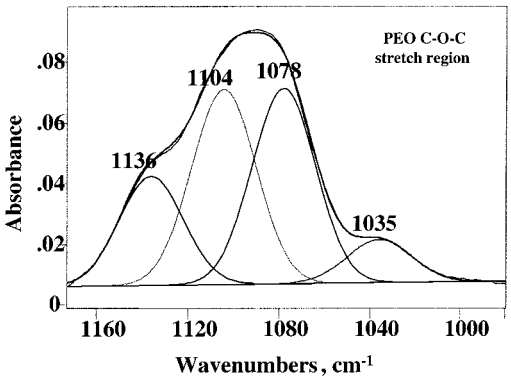

Figure 5. Infrared absorption spectrum of poly(ethylene oxide), PEO, at concentration 10 mg mL^{-1} in buffered D_2O solution at pH = 2 in the region of COC stretch vibrations and its spectral decomposition into component peaks. The pH = 2 was produced by 0.01 M HCl.

with widths of 23 and 24 cm^{-1} and the peaks centered at 1641 and 1658 cm^{-1} and one weaker peak of 29 cm^{-1} width and peak centered at 1622 cm^{-1}. The curve fitting gave consistent results when all the peaks used in the procedure were of Gaussian shape. The exact position of the low-wavenumber peak, determined by an experiment in which difference spectra were taken after a layer of PMAA was deposited on top of the film, is described in the section IR Analysis of Hydrogen Bonding.

It is important to note that spectra of PVPON solutions at pH = 2 (0.01 HCl) and pH = 8.4 (0.01 M phosphate buffer) were identical. This suggests that pyrrolidone rings were not protonated in acidic conditions.

3. Representative Spectra of PEO. Figure 5 shows the IR spectrum of a single PEO layer deposited on top of a PEO/PMAA multilayer film in the region of COC stretch vibrations. The broad band centered at 1088 cm^{-1} could be decomposed into four Gaussian peaks each with the peak width of 33 cm^{-1} (Figure 5). The peaks at 1104 and 1078 cm^{-1} were earlier assigned to symmetric and asymmetric COC stretch vibrations, respectively.[60] The peaks at 1136 and 1035 cm^{-1} also contained contributions from the CC stretch and CH_2 rocking vibrations; the detailed peak assignment can be found elsewhere[60,61] Though it is known that the spectral details in the COC stretching region give insight into the ether oxygen environment which should be distorted due to hydrogen bonding, we did not quantify this effect because of large uncertainties as-

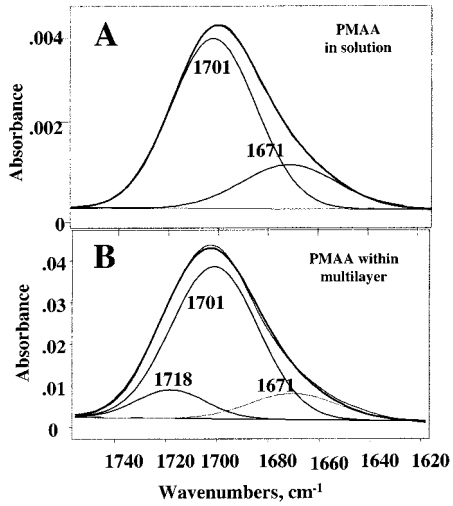

Figure 6. Comparison of the adsorption spectra of PMAA free in solution (panel A) and included into 10 layers of self-assembled PVPON/PMAA film (panel B). Conditions in panel A are the same as in Figure 4A. Mass deposited during layer-by-layer deposition of PVPON/PMAA multilayers is shown in Figure 2.

sociated with overlap of the contributions of PMAA vibrations to the spectra of PEO in the COC stretching region. These uncertainties did not significantly aggravate determination of the amount of PEO deposited in the multilayers and could introduce not more than 7% error into the latter calculation.

C. IR Analysis of Hydrogen Bonding. 1. Changes in the Carbonyl Region of Poly(carboxylic acid)s. After PMAA was included within a PEO/PMAA multilayer, the spectral features in the carbonyl region were modified (Figure 6). To quantify these changes, a third peak centered at 1718 cm^{-1} was added at the curve-fitting step. The exact position of this peak was determined in a control experiment, in which difference spectra were taken after deposition of two successive layers. This peak, presumably associated with the fraction of carboxyl groups bound with the ether groups of PEO, emerged as a small peak that accounted for only 5% of the total intensity of the carbonyl band. The peak assignment is in good agreement with known data on complexation of PMAA with PEO in cast films.[52] This assignment was further confirmed in a control experiment: when the multilayer was dried by flow of dry nitrogen gas, absorption at 1718−1720 cm^{-1} strongly increased, probably due to dehydration of the COOH−COC hydrogen bond.

Complexation of PMAA within a film was also accompanied by decrease in intensity of the low-frequency shoulder peak, from 20 to 22% of the total carbonyl peak intensity for the PMAA molecules in solution to only 14−15% within the PEO/PMAA film. This number took an intermediate value of 17−18% when PMAA was included into the top adsorbed layer. It is evident from this result that hydrogen bonding of −COOH with the ether group successfully competed with high-order self-association of carboxylic groups. However, we were unable to quantify the fraction of segments involved in hydrogen bonding because the extinction coefficient of the −COOH groups bound with the ether groups is unknown.

2. Changes in the Carbonyl Region of PVPON. As shown above, a weak peak centered at 1622 cm^{-1} should be introduced to account for a slight asymmetry

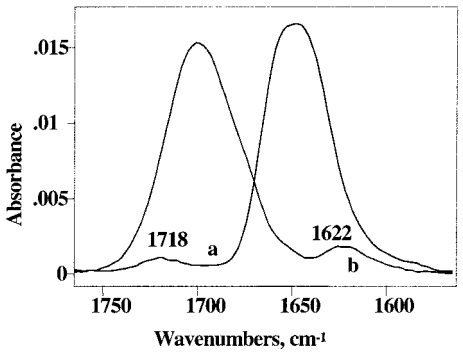

Figure 7. Infrared spectra of PVPON (a) and PMAA (b) deposited within a top layer at each successive step of assembly of a PVPON/PMAA multilayer, shown in Figure 1. Conditions are the same as in Figure 1.

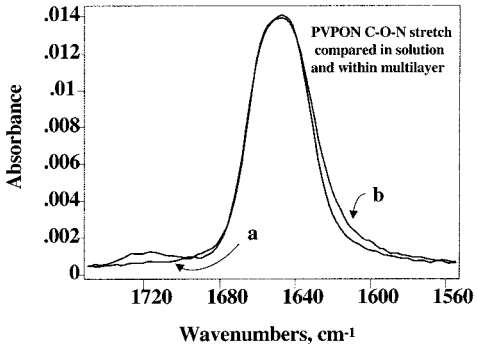

Figure 8. Comparison of the adsorption spectra of PVPON free in solution (a) and deposited within a top layer at each successive step of assembly of a PVPON/PMAA multilayer, shown in Figure 2b. Conditions are the same as in Figure 1.

of the PVPON infrared absorption in solution. After PVPON was included into the PVPON/PMAA multilayers, the intensity of this peak increased. This was shown by taking difference spectra after a layer of PMAA was deposited on top of the film. The data are shown in Figure 7b. Besides the characteristic strong band at 1700 cm^{-1}, which corresponds to the stretch vibrations of the C═O carbonyl groups of PMAA, one can see a weaker band centered at 1622 cm^{-1}. The latter band was missing in the spectra of PMAA in solution and comprised ∼8% of intensity of the PVPON in the multilayer.

Figure 8 shows changes of the PVPON spectrum after this polymer deposited on top of PMAA layer. A shoulder on the low-frequency side is evident. The low-wavenumber peak at 1622 cm^{-1} could account for this difference; it comprised 13% of the total carbonyl band intensity of PVPON complexed with PMAA compared to only 4% in the spectrum of the PVPON in solution.

The low-frequency 1622 cm^{-1} peak has been assigned to the hydrogen-bonded carbonyl groups in the PVPON molecules. This assignment agrees with findings made in other groups. Low-frequency shifts of the carbonyl stretch of PVPON after complexation with poly(carboxylic acid) in melts were reported elsewhere.[59] The origin of the residual low-frequency shoulder in the spectrum of PVPON in solution (Figure 4) is unclear, however. One possibility could be hydrogen bonding of the carbonyl moiety with the solvent molecules. Another scenario would involve association of carbonyl dipoles; this possibility was discussed above.

It was not feasible however to measure an increase in this low-frequency shoulder when PVPON molecules

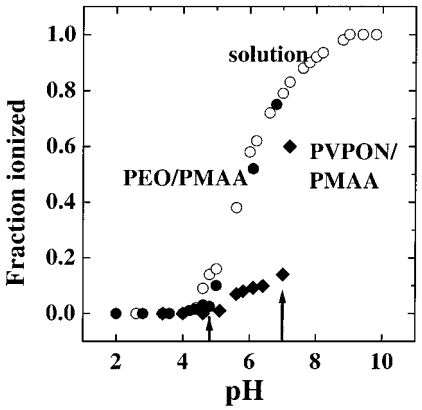

Figure 9. Comparison of ionization of PMAA free in solution (open circles) and included within PVPON/PMAA (diamonds) or PEO/PMAA multilayers (filled circles) at various pH. Assembly of PVPON/PMAA and PEO/PMAA multilayers was performed at pH = 2 and is shown in Figures 2 and 3. Critical pH values, above which multilayers dissolved at the rate grater than 0.15 mg min^{-1}, are marked by the arrows.

were "sandwiched" between layers of PMAA, owing to strong overlap of the bands which originate from C=O stretch vibrations in PMAA and uncertainty of how to subtract the PMAA contribution. But by using a simple argument of symmetry, this portion may be estimated as at least ~26% of the total intensity of PVPON vibrations in the carbonyl region.

At this point we cannot use these data to calculate the degree of hydrogen bonding between the polymeric species within the multilayer because an extinction coefficient of the bound PVPON segments is unknown. Below we will discuss an alternative approach to determine the amount of hydrogen bonds in the films. This approach will be based on the direct determination of ionization of polyacid within the multilayer.

Binding of PVPON with PMAA caused changes in the PMAA spectra similar to those in the PEO/PMAA system. In a similar way as in the PEO/PMAA system, a new peak at 1718 cm^{-1} emerged in the spectrum of PVPON after it was deposited on top of PMAA (Figures 8A). This peak originated from hydrogen bonding with PVPON. However, the changes in spectra of PMAA were hard to quantify further because of spectral overlap of PMAA and PVPON in the carbonyl region.

D. Estimate of Hydrogen Bonding Based on Measurements of Ionization. In this section, we are interested in an alternative approach to determine the amount of hydrogen bonding in the films. This approach will be based on the direct determination of ionization of polyacid molecules within the multilayer and comparison of this value with that measured for the solution. Figure 9 contrasts ionization of PMAA molecules free in solution and included within the multilayers at various pH. Ionization of PMAA in solution grew as a function of pH in a predictable way, consistent with the known ionization constants of the PMAA molecule.[62,63] Except at pH < 4.6, where PMAA was hardly ionized, ionization of carboxylic groups was significantly less within a PVPON/PMAA multilayer than in PMAA solution at any given pH. In contrast to the previously reported potentiomentric measurements of the fraction of hydrogen bonds between associating macromolecules,[46,64] our data present direct spectroscopic evidence of the consequences that hydrogen bonding has on molecular ionization.

It could be argued that suppressed ionization might stem from altered local dielectric environment within the film. The suppression of dissociation of ionizable groups if they are located in an environment of enhanced hydrophobicity is known in colloid chemistry and biochemistry.[65−67] However, data presented in Figure 9 for the PEO/PMAA films argue against this hypothesis. Ionization of carboxylic groups within the PEO/PMAA multilayer was only slightly less than in PMAA solution. It is reasonable to assume that the dielectric environment was not much different from that within PVPON/PMAA films. Instead, reduced ionization in these films was presumably rooted in hydrogen bonding of carboxylic groups with ether groups in PEO molecules or carbonyl groups of the PVPON ring.

Comparing the ionization degrees in Figure 9, we estimated the fraction of segments of carboxylic groups in the PMAA molecules that were involved in hydrogen bonding within the multilayer. This fraction was calculated as the difference between ionization of PMAA molecules in solution and in the film at a given pH. We conclude that a large fraction of COOH groups, from 40 to 50% in the pH range from 5.5 to 6.9, were bound within the PVPON/PMAA films. A much smaller fraction of PMAA functional groups, from 7 to 10% in the pH range from 4.4 to 4.9, was involved in intermolecular hydrogen bonding within the PEO/PMAA films. This is consistent with the data reported in the literature on relative stability of PVPON/PMAA and PEO/PMAA complexes in solution.[17,50] This is also in good agreement with the data in Figures 5 and 6.

E. Multilayers Are Destroyed at High pH. 1. Effects of Molecular Weight. PVPON/PMAA System. A unique aspect of this self-assembly method is reversibility: multilayers can be not just created but also destroyed. Figure 10 illustrates the controlled destruction, by change of the environmental pH, of the PVPON/PMAA multilayer. The molecular weight of the PVPON was ~1 300 000 g mol^{-1}. The self-assembly of this multilayer is illustrated in Figure 1. The top panel of Figure 10 shows the fraction of organic molecules retained at the surface, after 30 min of exposure of the multilayer to a buffer solution, plotted as a function of pH. One sees that the multilayer was stable up to pH = 6.9 but dissolved when the pH was raised above this point. The inset in Figure 10 shows that around this critical pH the rate at which the multilayer dissolved rose dramatically. At pH only 0.2 units smaller than 6.9, the multilayer dissolved extremely slowly, at the rate of ~0.01 mg m^{-2} min^{-1}. At pH only 0.2 units higher than 6.9, this rate was at least 100 times higher. The critical pH was defined as the pH corresponding to ~0.15 mg m^{-2} min^{-1} rate of loss of the amount deposited. It is evident, since the pH range for this transition was rather narrow, that this might have practical ramifications.

The bottom panel of Figure 10 points to the explanation of this effect. The multilayers dissolved because of negative electric charge, introduced into the multilayers by ionization of the carboxylic acid functionality in PMAA. At the critical point, as many as ~14% of PMAA groups were ionized. It is evident that when the pH was increased, repulsion between the ionized PMAA functional groups was counterbalanced by hydrogen bonds between PVPON and PMAA molecules, until a critical concentration of charge was approached and the multilayer "exploded".

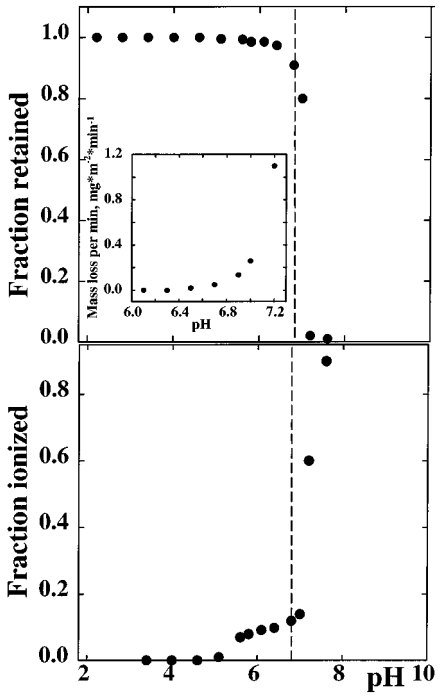

Figure 10. Illustration of pH sensitivity of a PVPON/PMAA multilayer whose assembly at low pH was illustrated in Figure 2. As a function of pH, the relative mass adsorbed after 30 min is plotted (top panel), and the percentage of ionized carboxylic acids within PMAA layers is plotted (bottom panel). Inset in top panel shows rate of disintegration of a multilayer at various pH. The units of disintegration are mass loss (mg m^{-2}) per minute.

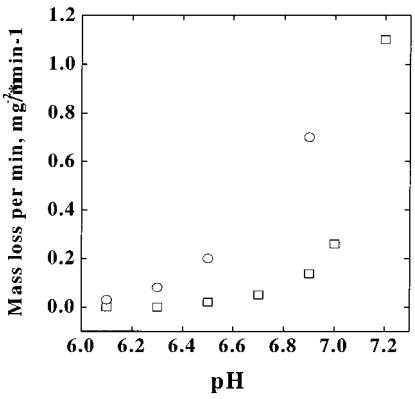

Figure 11. Comparison of rates of disintegration of a PVPON/PMAA multilayer for various molecular weight of PVPON molecules: ~1 300 000 g mol^{-1} (squares) or ~55 000 g mol^{-1} (circles). The assembly of PVPON/PMAA multilayers was performed at pH = 2. Saturated amounts deposited within each successive layer did not depend on molecular weight and are shown in Figure 1.

It is relevant to notice that stability of multilayers was also controlled by molecular weight of the polymers. Figure 11 shows that the critical pH was reduced about 0.4 units of pH when the molecular weight of PVPON was reduced from ~1 300 000 to ~55 000 g mol^{-1}. This effect was reasonable to expect, because the complexation energy per molecule was smaller for shorter PVPON molecules.

2. Effect of Chemical System. PEO/PMAA Multilayers. In this section, we intend to show that this critical pH, at which hydrogen-bonded multilayers fell apart owing to internal ionization, could be controlled by choice of the hydrogen-bonded chemical system.

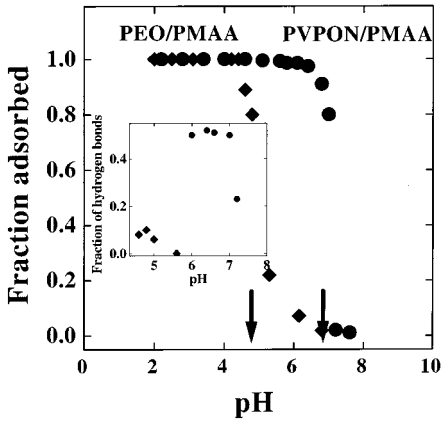

Figure 12. Comparison of pH-triggered disintegration of multilayers in the PVPON/PMAA (diamonds) and PEO/PMAA (circles) systems. Assembly of these multilayers is shown in Figures 2 and 3. Inset shows fraction of hydrogen bonding in these two systems, determined from the data in Figure 9. Arrows indicate the critical pH points, which separate regions of stable and unstable multilayers.

Figure 12 shows that this effect was large: it was pH = 6.9 in the PVPON system, but pH = 4.6 in the PEO/PMAA system. The inset in Figure 12 points to the explanation. The multilayers with a stronger amount of hydrogen bonds were more stable.

There are two ways in which hydrogen bonding affected the stability of multilayers. First, hydrogen bonding suppressed ionization of the PMAA functionality in the film at every pH. The stronger the hydrogen bonding in the film, the higher the pH at which a given ionization of PMAA groups was reached. Second, the extent of ionization that a film would tolerate while still remaining intact depended on the strength of hydrogen bonding. This is because the critical point was determined by the tradeoff between emerging electrostatic electrostatic repulsions and hydrogen bonding. The PVPON/PMAA complexes were strongest and could tolerate up to ~14% ionization of PMAA, but those formed from the pairing of PMAA and PEO dissolved when ionization of PMAA was as low as ~2−3%.

It was meaningful to calculate the average spacing between two charges in the multilayer at this critical ionization. On the basis of a procedure that we described previously,[68] we found that the average charge−charge spacing was ~10 Å in the PVPON/PMAA system and ~27 Å in the PEO/PMAA system. It is evident that stronger hydrogen bonding reduced the critical distance, between charges, at which multilayers lost stability.

3. PEO/PAA Multilayers. The self-assembly of PEO/PAA multilayers was performed the same way as for the PEO/PMAA system. Characteristics of the multilayers deposited at pH = 2 were very similar in these two systems, though significant conformational differences for PMAA and PAA molecules in solution are known.[62,69] However, the pH stability of multilayers containing these two molecules was very different. This is shown in Figure 13, where the relative mass retained is plotted as a function of pH. One sees that the critical pH was ~3.6 in the PEO/PAA multilayers, about one unit of pH lower than in the PEO/PMAA system. At the same time, multilayers were able to tolerate the same fraction of ionized carboxylic groups, about 2−3%. This suggests that strength of hydrogen bonding of both polyacids with PEO ether groups was similar. Instead, the lower critical pH in the PEO/PAA system is con-

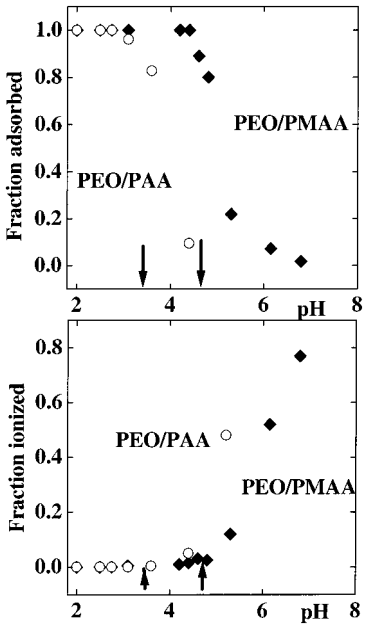

Figure 13. Comparison of pH-triggered disintegration of multilayers in the PEO/PMAA and PEO/PAA systems. The assembly of a PEO/PMAA multilayer is shown in Figure 2. Deposition of a PEO/PAA multilayer, performed in a similar way, is not shown. Inset shows the degree of hydrogen bonding in these two systems, determined from the data in Figure 9. Arrows indicate critical pH points, which determined stability boundary of the multilayers.

sistent with the known[62,63,70] stronger acidity of PAA molecules. This same effect is seen in bulk solutions as illustrated above for ionization of PAA and PMAA molecules as a function of pH.

We further found that when carboxylic groups were "diluted" within a polymer chain (as in a random copolymer of acrylamide and acrylic acid with 20% of acrylic acid units), growth of multilayers was completely inhibited. Probably this is because acrylamide units, which did not interact with PEO molecules and therefore created "defects" along a chain, were so abundant in this copolymer. The copolymer used in this experiment had a molecular weight of ~200 000; it was purchased from Sigma-Aldrich.

4. Effect of the Ionic Strength on the Film Stability. The stability of multilayer hydrogen-bonded films could also be controlled by ionic strength. Figure 14 shows the effect of ionic strength on kinetics of disintegration of the PEO/PMAA film. After the multilayer was self-assembled at acidic pH, it was exposed to an 0.01 M phosphate buffer at pH = 5.15, which is higher than the critical pH = 4.6. The total mass of the organic film deposited on the crystal decreased rapidly with elapsed time (Figure 14). Buffer solution was then exchanged to another buffer solution at the same pH but containing 0.4 M NaCl. Dissolution of the multilayer was completely inhibited in this condition. The reason is that a higher ionic strength reduces the intensity of electrostatic repulsion between a given number of ionized groups within a multilayer assembly. Such an effective screening effect also suggests that the films were permeable to the small ions.

It is also interesting to notice that at high concentration of salt the quantity of ionized carboxylic groups within the film increased from 4 to 13% but that these additional charges apparently were also efficiently screened by the small ions. To quantify this effect, it

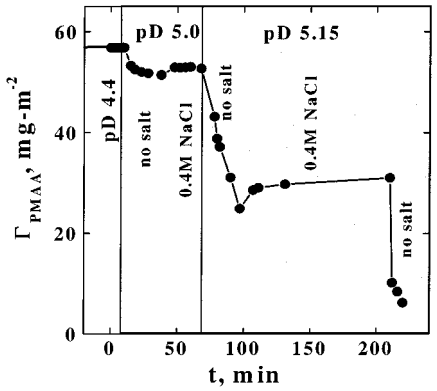

Figure 14. Time evolution of total mass deposited within a PEO/PMAA multilayer when buffer solution at pH = 5.15 with 0.01 M ions supplied by phosphate buffer was replaced with the same buffer solution but with 0.4 M NaCl and then again by the original buffer. Deposition of the PEO/PMAA layers, performed at low pH, is shown in Figure 2.

was instructive to calculate spacing between charges within the multilayer assembly. This spacing was ~25 Å in the unstable PEO/PMAA film in the environment of 10 mM ions, and it was ~10 Å in the environment of 0.4 M NaCl, where the film was stable. The ratio of these spacings was less than the ratio of the electrostatic Debye screening lengths at these ion concentrations, which was equal to 6.3. This difference explains the stabilization effect.

5. Inclusion of Rhodamine 6G Molecule into the Multilayer and Demonstration of Its Release. Although this work is still a long way from practical application, the concept can be used to design the deliberate release of foreign elements, such as drugs and dyes, that have been included within these layers. This concept builds upon studies of the takeup of drugs within interpolymer complex in solution.[71] We have confirmed this expectation by studying release of rhodamine 6G, a dye molecule, from PEO/PMAA multilayers. Adsorption of dye molecules into multilayers was easy to follow by the intense characteristic vibrations in the region 1250−1650 cm^{-1} (the strongest band was centered at 1606 cm^{-1}).

Deposition of dye/PEO/PMAA miltilayers was performed by a method similar to that described in the section for the PEO/PMAA system, except for two details. First, prior to deposition, filtered rhodamine 6G solution at 0.5 mg/mL was mixed with PMAA solution (concentration of dye in the resultant solution was 0.25 mg/mL). Second, since preliminary experiments showed ~20 times more dye to deposit within multilayers at pH = 4 (rather than at pH = 2 as in experiments discussed above), we performed deposition at this higher pH. This is probably because PMAA molecules became slightly ionized at pH = 4 and interacted more strongly with positively charged dye molecules. We observed a systematic growth of the PEO/PMAA multilayer, with incremental mass increases of ~6.5 mg m^{-2} for PMAA and ~4 mg m^{-2} for PEO. It was difficult to quantify the amount of dye included into the multilayers because the extinction coefficient of rhodamine 6G was not known. The films were of intense pink color, and no dye was desorbed into solution even after rinsing with large amounts of buffer at pH = 4. However, when the films were exposed to a buffer solution of the same ionic strength but higher pH = 5.5, the surface-bound layers were completely dissolved and the solution turned

bright pink. This admittedly qualitative test shows the feasibility of this method for release technology.

Acknowledgment. This work was supported by the taxpayers of the United States by the U.S. Department of Energy, Division of Materials Science, through Grant DEFG02-91ER45439 to the Frederick Seitz Materials Research Laboratory at the University of Illinois at Urbana−Champaign.

References and Notes

(1) Esker, A. R.; Mengel, C.; Wegner, G. *Science* **1998**, *280*, 892.
(2) Caruso, F.; Caruso, R. A.; Möhwald, H. *Science* **1998**, *282*, 1111.
(3) Shiratori, S. S.; Rubner, M. F. *Macromolecules* **2000**, *33*, 4213.
(4) Clark, S. L.; Hammond, P. T. *Adv. Mater.* **1998**, *10*, 1515.
(5) Husemann, M.; Morrison, M.; Benoit, D.; Frommer, K. J.; Mate, C. M.; Hinsberg, W. D.; Hedrick, J. L.; Hawker, C. J. *J. Am. Chem. Soc.* **2000**, *122*, 1844.
(6) Xia, Y. N.; Whitesides, G. M. *Annu. Rev. Mater. Sci.* **1998**, *28*, 153.
(7) Huck, W. T. S.; Stroock, A. D.; Whitesides, G. M. *Angew. Chem., Int. Ed.* **2000**, *39*, 1058.
(8) Decher, G.; Hong, J.-D. *Macromol. Chem., Macromol. Symp.* **1991**, *46*, 321.
(9) Decher, G. *Science* **1997**, *277*, 1232.
(10) Lvov, Yu.; Haas, H.; Decher, G.; Möhwald, H.; Mikhailov, A.; Mtchedlishvily, B.; Morgunova, E.; Vainshtein, B. *Langmuir* **1994**, *10*, 4232.
(11) Cheung, J. H.; Stockton, W. B.; Rubner, M. F. *Macromolecules* **1997**, *30*, 2712.
(12) Schlenoff, J. B.; Ly, H.; Li, M. *J. Am. Chem. Soc.* **1998**, *120*, 7626.
(13) Caruso, F.; Lichtenfeld, H.; Giersig, M.; Möhwald, H. *J. Am. Chem. Soc.* **1998**, *120*, 8523.
(14) Donath, E.; Sukhorukov, G. B.; Caruso, F.; Davis, S. A.; Möhwald, H. *Angew. Chem., Int. Ed. Engl.* **1998**, *37*, 2202.
(15) Antipina, A. D.; Baranovskii, V. Yu.; Papisov, I. M.; Kabanov, V. A. *Polym. Sci. U.S.S.R.* **1972**, *A14*, 1047.
(16) Baranovsky, V. Yu.; Litmanovich, A. A.; Papisov, I. M.; Kabanov, V. A. *Eur. Polym. J.* **1981**, *17*, 969 and references within.
(17) Tsuchida, E.; Abe, K. *Adv. Polym. Sci.* **1982**, *45*, 1.
(18) Philippova, O. E.; Karibyants, N. S.; Starodubtzev, S. G. *Macromolecules* **1994**, *27*, 2398.
(19) Krische, M. J.; Lehn, J. M.; Kyritsakas, N.; Fischer, J. *Helv. Chim. Acta* **1998**, *81*, 1909.
(20) Kato, T.; Fréchet, J. M. J. *Macromolecules* **1989**, *22*, 3818.
(21) Kwon, I. C.; Bae, Y. H.; Kim, S. W. *Nature* **1991**, *354*, 291.
(22) Yoo, D.; Shiratori, S. S.; Rubner, M. F. *Macromolecules* **1998**, *31*, 4309.
(23) Muller, M.; Rieser, T.; Lunkwitz, K.; Berwald, S.; Meier-Haack, J.; Jehnichen, D. *Macromol. Rapid Commun.* **1998**, *19*, 333.
(24) Chen, K. M.; Jiang, X. P.; Kimerling, L. C.; Hammond, P. T. *Langmuir* **2000**, *16*, 7825.
(25) Xie, A. F.; Granick, S. *J. Am. Chem. Soc.* **2001**, *123*, 3175.
(26) Dubas, S. T.; Farhat, T. R.; Schlenoff, J. B. *J. Am. Chem. Soc.* **2001**, *123*, 5368.
(27) Cao, T.; Chen, J.; Yang, Ch.; Cao, W. *Macromol. Rapid Commun.* **2001**, *22*, 181.
(28) Stockton, W. B.; Rubner, M. F. *Macromolecules* **1997**, *30*, 2717.
(29) Wang, L. Y.; Wang, Z. Q.; Zhang, X.; Shen, J. C.; Chi, L. F.; Fucks, H. *Macromol. Rapid Commun.* **1997**, *18*, 509.
(30) Wang, L. Y.; Fu, Y.; Wang, Z. Q.; Fan, Y.; Zhang, X. *Langmuir* **1999**, *15*, 1360.
(31) Sukhishvili, S. A.; Granick, S. *J. Am. Chem. Soc.* **2000**, *122*, 9550.
(32) Dubas, S. T.; Schlenoff, J. B. *Macromolecules* **2001,** *34*, 3736.
(33) Boils, D.; Hair, M. L. *J. Colloid Interface Sci.* **1993**, *157*, 19.
(34) Devanand, K.; Selser, J. C. *Nature* **1990**, *343*, 739.
(35) Devanand, K.; Selser, J. C. *Macromolecules* **1991**, *24*, 5943.
(36) Fuoss, R. M.; Strauss, U. P. *J. Polym. Sci.* **1948**, *3*, 246.
(37) Margolin, A. L.; Izumrudov, V. A.; Švedas, V. K.; Zezin, A. B.; Kabanov, V. A.; Berezin, I. V. *Biochim. Biophys. Acta* **1981**, *660*, 359.
(38) Frantz, P.; Granick, S. *Macromolecules* **1995**, *28*, 6915.
(39) Peanasky, J.; Schneider, H. M.; Granick, S.; Kessel, C. R. *Langmuir* **1995**, *11*, 953.
(40) Frantz, P.; Granick, S. *Langmuir* **1992**, *8*, 1176.
(41) Johnson, H. E.; Granick, S. *Macromolecules* **1990**, *23*, 3367.
(42) Sukhishvili, S. A.; Granick, S. *J. Chem. Phys.* **1998**, *109*, 6861.
(43) Bimendina, L. A.; Tleubayeva, G. S.; Bekturov, Ye. A. *Vysokomol. Soyed.* **1977**, *A19*, 71.
(44) Iliopoulos, I.; Audebert, R. *Eur. Polym. J.* **1988**, *24*, 171.
(45) Higashi, N.; Matsumoto, T.; Niwa, M. *Langmuir* **1994**, *10*, 4651.
(46) Osada, Y. *J. Polym. Sci., Polym. Chem. Ed.* **1979**, *17*, 3485.
(47) Bailey, F. R., Jr.; Lundberg, R. D.; Callard, R. W. *J. Polym. Sci.* **1964**, *A2*, 845.
(48) Papisov, I. M.; Baranovkii, V. Yu.; Sergieva, Ye. I.; Antipina, A. D.; Kabanov, V. A. *Polym. Sci. U.S.S.R.* **1974**, *A16*, 1311.
(49) Papisov, I. M.; Nedyalkova, Ts. I.; Avramchuk, N. K.; Kabanov, V. A. *Polym. Sci. U.S.S.R.* **1973**, *A15*, 2259.
(50) Abe, K.; Koide, M.; Tsuchida, E. *Macromolecules* **1977**, *10*, 1259.
(51) Lee, J. Y.; Painter, P. C.; Coleman, M. M. *Macromolecules* **1988**, *21*, 346.
(52) Lu, X.; Weiss, R. A. *Macromolecules* **1995**, *28*, 3022.
(53) Dong, J.; Ozaki, Y.; Nakashima, K. *Macromolecules* **1997**, *30*, 1111.
(54) Trewhella, J.; Liddle, W. K.; Heidorn, D. B.; Strynadka, N. *Biochemistry* **1989**, *28*, 1294.
(55) Maura, J. J.; Eustance, D. J.; Ratcliffe, C. T. *Macromolecules* **1987**, *20*, 196.
(56) Painter, P. C.; Pehlert, G. J.; Hu, Y. H.; Coleman, M. M. *Macromolecules* **1999**, *32*, 2055.
(57) Sasaki, N.; Yokoyama, T. *Kobunshi Ronbunshu* **1984**, *41*, 9.
(58) Takayama, K.; Nagai, T. *Chem. Pharm. Bull.* **1987**, *35*, 4921.
(59) Yaung, J.-F.; Kwei, T. K. *J. Appl. Polym. Sci.* **1998**, *69*, 921.
(60) Enriquez, E. P.; Granick, S. *Colloids Surf, A* **1996**, *113*, 11.
(61) Zalewska, A.; Wieczorek, W.; Stevens, J. J. R. *J. Phys. Chem.* **1996**, *100*, 11382.
(62) Jager, J.; Engberts, J. B. F. N. *Pays-Bas* **1986**, *105*, 347.
(63) Ikawa, T.; Abe, K.; Honda, K.; Tsuchida, E. *J. Polym. Sci., Polym. Chem. Ed.* **1975**, *13*, 1505.
(64) England, D.; Crowther, N. J.; Butler, C. J. *Eur. Polym. J.* **1994**, *30*, 767.
(65) Sukhishvili, S. A.; Chechik, O. S.; Yaroslavov, A. A. *J. Colloid Interface Sci.* **1996**, *178*, 42.
(66) Dyson, H. J.; Jeng, M. F.; Model, P.; Holmgren, A. *FEBS Lett.* **1994**, *339* (1−2), 11.
(67) Lamm, G.; Pack, G. R. *Int. J. Quantum Chem.* **1997**, *65*, 1087.
(68) Sukhishvili, S. A.; Granick, S., submitted for publication.
(69) Morawetz, H. *Macomolecules* **1996**, *29*, 2689.
(70) Spencer, H. G. *J. Polym. Sci.* **1962**, *56*, S25.
(71) Aksenova, N. I.; Kemenova, V. A.; Kharenko, A. V.; Zezin, A. B.; Bravova, G. B.; Kabanov, V. A. *Polym. Sci. U.S.S.R.* **1998**, *A40*, 226.

MA011346C